Nonsingular walls in plane cholesteric layers



2006 J. Phys.: Condens. Matter 18 4443

(http://iopscience.iop.org/0953-8984/18/19/001)

INSTITUTE OF PHYSICS PUBLISHING JOURNAL OF PHYSICS: CONDENSED MATTER

J. Phys.: Condens. Matter **18** (2006) 4443–4460 doi:10.1088/0953-8984/18/19/001

# Nonsingular walls in plane cholesteric layers

**V A Belyakov[1], M A Osipov[2] and I W Stewart[2]**

[1] Landau Institute for Theoretical Physics, Kosygin Street 2, 117334 Moscow, Russia
[2] Department of Mathematics, University of Strathclyde, Livingstone Tower, 26 Richmond Street, Glasgow G1 1XH, UK

Received 26 December 2005
Published 25 April 2006
Online at stacks.iop.org/JPhysCM/18/4443

**Abstract**

The structure of a straight interface (wall) between regions with differing values of the pitch in planar cholesteric layers with finite strength of the surface anchoring is investigated theoretically. It is found that the shape and strength of the anchoring potential influences essentially the structure of the wall and a motionless wall between thermodynamically stable regions without a singularity in the director distribution in the layer can exist for sufficiently weak anchoring only. More specifically, for the existence of such a wall the dimensionless parameter $S_d = K_{22}/Wd$ (where $W$ is the depth of the anchoring potential, $K_{22}$ is the elastic twist modulus and $d$ is the layer thickness) should exceed its critical value, which is dependent on the shape of the anchoring potential. General equations describing the director distribution in the wall are presented. Detailed analysis of these equations is carried out for the case of infinitely strong anchoring at one surface and finite anchoring strength at the second layer surface. It is shown that the wall width $L$ is directly dependent upon the shape and strength of the anchoring potential and that its estimate ranges from $d$ to $(dL_p)^{1/2}$ (where $L_p = K_{22}/W$ is the penetration length), corresponding to different anchoring strengths and shape potentials. The dependence of the director distribution in the wall upon all three Frank elastic moduli is analytically found for some specific limiting cases of the model anchoring potentials. Motion of the wall is briefly investigated and the corresponding calculations performed under the assumption that the shape of a moving wall is the same as a motionless one. It is noted that experimental investigation of the walls in planar cholesteric layers can be used for the determination of the actual shape of surface anchoring potentials.

## 1. Introduction

The dynamics of chiral liquid crystal pitch jumps in planar layers with a finite surface anchoring strength now attracts considerable attention due to the interesting physics of the phenomenon [1, 2] and its direct connection to liquid crystal applications [3]. The jump of the pitch in the cell initiated by a smooth variation of some external parameter (temperature,

  

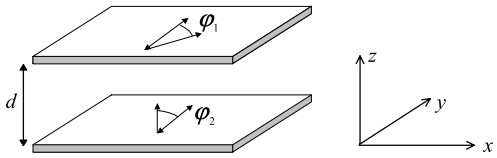


**Figure 1.** The case of nonidentical anchoring at the surfaces of a cholesteric layer. The $z$ axis is normal to the layer and is in the direction of the helical axis. The alignment direction is along the $y$ axis while the $x$ axis determines the direction of any wall motion that may be present.

electric or magnetic field etc) may occur simultaneously in a whole cell [1, 2] or as a jump in a limited area of the cell, with a further spreading of this area over the whole cell [4, 5]. The velocity of this spreading is directly dependent on the shape and strength of the surface anchoring potential and on the director distribution in the intermediate region of the layer (wall) between the initial and final values of the pitch in the course of a jump [5]. Up until now there have been no investigations of the director distribution in the wall between regions of different values of the pitch in the case of relatively weak surface anchoring. For example, in the case of similar walls in a Cano wedge, only those walls with a singularity in the director distribution are mentioned [6, 7]. The director distribution in a straight motionless wall will be theoretically investigated below and its connection with the strength and shape of surface anchoring potentials will be revealed. Note that the wall may be motionless if the free energies of the director configurations in the layer over a unit area of the layer on both sides of the wall are exactly the same. Otherwise, the straight wall will experience a motion with constant velocity in a direction where the free energy per unit area of the layer is higher [5]. The shapes found below for the motionless wall are dependent on the shape of the anchoring potential and may be useful for the reconstruction of the actual surface anchoring potential and for a study of the jump dynamics because, naturally, for low velocities of the wall motion it retains almost the same shape as the motionless one.

### *1.1. General results*

Before discussing the main problem of this paper, we recall briefly the starting point for pitch jump investigations for a planar cholesteric layer with a finite surface anchoring strength. Specifically, we shall examine the temperature behaviour of the cholesteric helix in a planar cholesteric layer of finite thickness with a finite anchoring strength at one of its surfaces and infinite anchoring at the other (see figure 1). We restrict the analysis of the temperature variations of the director configuration in the layer by the assumptions that the pitch jump mechanism is connected with the director overcoming the anchoring barrier at the surface and, moreover, that liquid crystal thermal fluctuations may be neglected. The main attention in the investigation below, following the approach of [1, 8], will concentrate on the transitions between $N$ and $N+1$ half-turns of the director in the layer, which proceed without strong local disturbances of the director configuration. The analysis of the problem (see [1, 8]) shows that in a layer with homogeneous distribution of the director over the layer surface a smooth change with temperature of the director deviation angle from the alignment direction $\varphi$ is possible while $\varphi$ is less than some critical angle $\varphi_c$. Upon $\varphi$ achieving the critical value $\varphi_c$, a jump-like change of the pitch occurs and a transition to a new configuration of the helix takes place, differing by one in the number of half-turns $N$. The critical value $\varphi_c$ corresponds to the configuration with $N$ director half-turns in the layer achieving an instability point and a reduction to zero in the potential barrier between the two director configurations with $N$ and $N+1$ half-turns.

If the described jump occurs in a limited area of the layer surface the director distribution over the layer surface becomes inhomogeneous and the wall (the interface between the configurations with $N$ and $N+1$ half-turns of the director) begins its motion in the direction of the $N$ configuration, because the free energy of the $N$ configuration per unit layer area is higher than the corresponding value for the $N+1$ configuration.

Since, generally speaking, the moving and motionless walls are different, in order to formulate the problem for a motionless wall we have to accept that the free energy of the $N$ configuration per unit layer area is the same as the corresponding free energy of the $N+1$ configuration. This situation occurs when the director deviation angle $\varphi$ is less than the critical angle $\varphi_c$. Therefore we have to find, for a homogeneous layer, the value of the angle, which we shall call $\varphi_e$, for which the free energy of the $N$ configuration per unit layer area is the same as the corresponding free energy of the $N+1$ configuration. For this purpose we have to use the expression for the free energy per unit area of a homogeneous layer given by [1, 8]

$$F(T) = W_s(\varphi) + \frac{K_{22}}{2d}\,[\varphi - \varphi_0(T)]^2\,, \tag{1.1}$$

where $W_s(\varphi)$ is the surface anchoring potential, $K_{22}$ is the elastic twist modulus, $d$ is the layer thickness and the angle $\varphi_0(T)$ gives the angle of the director deviation from the alignment direction at the surface with finite anchoring if the anchoring at this surface were absent, i.e., it is the free rotation angle determined by the temperature variations of the pitch in a bulk cholesteric sample. The free energies of the $N$ and $N+1$ configurations are equal for $\varphi_0(T) = \pi/2$. Thus the minimum of the free energy $F$ presented by equation (1.1) at $\varphi_0(T) = \pi/2$ determines the angle $\varphi_e$. For the $N+1$ configuration the corresponding angle is $-\varphi_e$. Now we can formulate the boundary conditions for the motionless wall where the director orientations at the layer surfaces far from both of the wall sides are given by the corresponding angles $\varphi_e$ and $-\varphi_e$. The transition along the layer surface from $\varphi_e$ to $-\varphi_e$ should proceed at a finite distance, otherwise it will be connected with a very high energy which is associated with the gradient of the pitch along the surface.

To determine the thickness of the wall and the director distribution in the wall one has to investigate the problem starting from the general expression for the density of the free energy of a cholesteric [6, 7], namely,

$$F_v = \tfrac{1}{2}K_{11}(\operatorname{div}\mathbf{n})^2 + \tfrac{1}{2}K_{22}(\mathbf{n}\cdot\operatorname{curl}\mathbf{n} + q_0)^2 + \tfrac{1}{2}K_{33}(\mathbf{n}\times\operatorname{curl}\mathbf{n})^2, \tag{1.2}$$

which does not assume, contrary to the situation in (1.1), that the distribution of the director $\mathbf{n}$ is homogeneous over the layer surface. Since we are considering a straight wall, all quantities in the problem are dependent on the coordinate along the layer surface being perpendicular to the wall (which we shall set to be the $x$-coordinate). Inside the layer the quantities are also dependent on the coordinate along the $z$-axis, which is perpendicular to the layer surface, with $z = 0$ corresponding to the layer surface with an infinitely strong anchoring and $z = d$ corresponding to the layer surface with a finite anchoring. In this frame the director $\mathbf{n}$ at some point in the layer depth is represented by the coordinate of this point as $(\cos\psi(z), \sin\psi(z), 0)$, where $\psi(z)$ is the angle between the director at the point $z$ and the alignment direction at the layer surface with an infinitely strong anchoring expressed via the local value of the pitch $p(x)$, depending on $x$, in the layer as

$$\psi(z) = \frac{2\pi}{p(x)}\,z. \tag{1.3}$$

The density of the free energy (1.2) in the same frame takes the form

$$F_v = \frac{1}{2}\left\{\left(\frac{\mathrm{d}\psi}{\mathrm{d}x}\right)^2\left[K_{11}\sin^2\psi + K_{33}(1+\cos^2\psi)\cos^2\psi\right] + K_{22}\left(\frac{\mathrm{d}\psi}{\mathrm{d}z} - q_0\right)^2\right\}. \tag{1.4}$$

For simplicity in equation (1.4) we do not explicitly show that the director orientation is a function of $x$ and $z$, i.e., $\psi = \psi(x, z)$.

To obtain the free energy per unit area of the layer one has to perform integration over the layer thickness in (1.4) and add the surface anchoring energy. Finally, one obtains the free energy per unit area of the layer with varying pitch $F(T)_i$:

$$F(T)_i = W_s(\varphi) + \frac{K_{22}}{2d}[\varphi - \varphi_0(T)]^2 + \frac{1}{2}\int \left(\frac{d\psi}{dx}\right)^2 \left[K_{11}\sin^2\psi + K_{33}(1+\cos^2\psi)\cos^2\psi\right] dz. \tag{1.5}$$

For simplification of (1.5) one has to take into account that in the case of infinitely strong anchoring at one surface of the layer there are very simple relationships following from (1.3) between the director orientation at the surface and in the bulk of the layer:

$$\psi(x, z) = \frac{z}{d}\varphi(x) \qquad \text{and} \qquad \frac{d\psi}{dx} = \frac{z}{d}\frac{d\varphi}{dx}. \tag{1.6}$$

By inserting (1.6) into (1.5) one obtains the free energy per unit area of the layer expressed via the director deviation angle at the layer surface:

$$F(T)_i = W_s(\varphi) + \frac{K_{22}}{2d}[\varphi - \varphi_0(T)]^2 + K_w\frac{d}{2}\left(\frac{d\varphi}{dx}\right)^2, \tag{1.7}$$

where the effective elastic modulus $K_w$ is given by the expression

$$K_w = \frac{1}{d}\int \left(\frac{z}{d}\right)^2 \left[K_{11}\sin^2\psi + K_{33}(1+\cos^2\psi)\cos^2\psi\right] dz, \tag{1.8}$$

where the angle $\psi$ is determined by equation (1.6). The expression in equation (1.8) for the effective elastic modulus $K_w$ is slightly dependent on $x$ due to the dependence of the director angle upon $x$ at the layer surface. However, if the number of director half-turns at the layer thickness is sufficiently large then one may neglect this dependence and, with a good degree of accuracy, accept the following expression for $K_w$:

$$K_w = \tfrac{1}{6}K_{11} + \tfrac{7}{24}K_{33}. \tag{1.9}$$

In the one constant approximation $K_{11} = K_{22} = K_{33} = K$, equation (1.9) reduces to

$$K_w = \tfrac{11}{24}K. \tag{1.10}$$

Applying the variational approach to the minimization of the free energy for the whole layer, with the free energy per unit area of the layer given by equation (1.7), one obtains the following equation determining the director distribution in the wall if the approximation for coordinate-independent $K_w$ is accepted:

$$\frac{d}{d\varphi}W_s(\varphi) + \frac{1}{d}K_{22}[\varphi - \varphi_0(T)] - K_w d\frac{d^2\varphi}{dx^2} = 0. \tag{1.11}$$

It can readily be shown that equation (1.11) has the following first integral:

$$F - K_w\frac{d}{2}\left(\frac{d\varphi}{dx}\right)^2 = C, \tag{1.12}$$

where $F$ is the free energy (1.1) and $C$ is a constant. The constant $C$ can be determined by considering equation (1.12) far from the wall where the derivative $d\varphi/dx$ vanishes. One obtains $C = F[\varphi = \varphi_{e1}] = F[\varphi = \varphi_{e2}] = F_c$ where $\varphi_{e1}$ and $\varphi_{e2}$ are the equilibrium angles at the surface on both sides of the wall (in the limit as $x = \pm\infty$). It should be stressed that the free energy density $F$ in the two regions separated by the wall (sufficiently far from the

wall) should be the same. Only in this case is the first integral defined. If the free energies are different, then the whole system is no longer in equilibrium and the planar wall will move with a certain velocity $v$, as will be discussed below.

From equation (1.12) one obtains

$$\frac{\mathrm{d}\varphi}{\mathrm{d}x} = \pm\left[\frac{2(F - F_c)}{K_w d}\right]^{\frac{1}{2}}. \tag{1.13}$$

It is convenient to set $x = 0$ in the middle of the wall and to change the variable in such a way that the 'shifted' angle $\Phi = 0$ is in the middle of the cell, i.e. for $x = 0$. Clearly, $\Phi = \varphi - (\varphi_{e1} + \varphi_{e2})/2$. Then the positive sign in equation (1.13) can be selected if one assumes that $\varphi_{e1} < \varphi_{e2}$. In this case the angle $\varphi(x)$ is an increasing function of $x$ for all $x$. Using the new variables, equation (1.13) can now be rewritten in the form

$$\frac{\mathrm{d}\Phi}{\mathrm{d}x} = \left[\frac{2(F(\Phi + \overline{\varphi}_c) - F_c)}{K_w d}\right]^{\frac{1}{2}} \tag{1.14}$$

where $\overline{\varphi}_c = (\varphi_{e1} + \varphi_{e2})/2$. One notes that the free energy $F$ now depends on $\Phi + \overline{\varphi}_c$ because the free energy (1.1) is not invariant under such a transformation in its argument.

Integration of equation (1.14) results in the following relation between the coordinate $x$ and the angle $\Phi$:

$$x = \int_0^{\Phi}\left[\frac{2(F(\hat{\Phi} + \overline{\varphi}_c) - F_c)}{K_w d}\right]^{-\frac{1}{2}} \mathrm{d}\hat{\Phi}, \tag{1.15}$$

where we have taken into account that $\Phi = 0$ when $x = 0$. One notes that (1.15) determines the natural scale for the variable $x$. Indeed, normalizing the free energy by the anchoring strength $W$ (on the right-hand side of (1.15)), equation (1.15) can be rewritten in the following dimensionless form:

$$X = \int_0^{\Phi}\left[2(\overline{F}(\hat{\Phi} + \overline{\varphi}_c) - \overline{F}_c)\right]^{-\frac{1}{2}} \mathrm{d}\hat{\Phi}, \tag{1.16}$$

where $\overline{F} = F/W$ and the dimensionless coordinate $X = x/L$, where the characteristic length $L = (W/K_w d)^{-1/2}$. Thus one concludes that the actual mathematical form of the profile $\Phi(X)$ inside the wall does not depend on the parameter $K_w$. This parameter only determines the scale of $x$. It follows also that in dimensional terms the width of the wall (for whatever definition) is proportional to $L$, i.e. the width $L_w = Ll_w$ where the dimensionless quantity $l_w$ does not depend on $K_w$. The integral in equation (1.16) can be evaluated numerically to express the dependence of the angle $\Phi$ upon $X$ for different forms of the anchoring potential. In the next section we present a number of numerical solutions for different values of the parameters and consider a simple analytical approximation for these solutions which will be used below to obtain approximate analytical results.

### *1.2. Anchoring and director distribution in the wall*

In order to analyse the above results it is important to consider the influence of different terms in equation (1.11) on the profile of the wall. Indeed, the last term in (1.11) can be estimated as $WS_w(d/L_w)^2$ where $L_w$ is the width of the wall and $S_w = K_w/Wd$ is a second dimensionless parameter similar to $S_d$, which is defined by $S_d = K_{22}/Wd$. The second term can be estimated as $WS_d$ and the first term can be estimated as $W$. For typical liquid crystal materials the effective elastic constant $K_w$ (given by equation (1.9)) and the twist elastic constant $K_{22}$ are of the same order [6], and therefore $S_w \propto S_d$. Taking into account that the width of the wall

is much smaller than the cell thickness $d$ (which follows both from experiments and from the numerical profiles that can be calculated from equation (1.16)) one concludes that the ratio of the third and the second terms in equation (1.11) is of the order $(d/L_w)^2 \gg 1$, i.e. the third term is predominant over the second one inside the wall. At the same time, the first term in (1.11) is also predominant over the second one whenever $S_w \ll 1$, i.e. in the case of strong anchoring. Thus one may consider a simple limiting case of sufficiently strong anchoring when the second term in equation (1.11) may be neglected. In this case one also has to neglect the corresponding term in the free energy (1.1). Consequently, the equilibrium angles on both sides of the wall are given by the simple asymptotic equation $dW_s/d\varphi = 0$. For the Rapini–Papoular potential in the form $W_s(\varphi) = -W\cos(2\varphi)$ one obtains the equation $\sin(2\varphi) = 0$ which has the solutions 0 and $\pi$ (the solution $\pi/2$ is unstable). This simply means that for sufficiently strong anchoring the equilibrium director at the surface is approximately parallel to the easy axis. For large but finite anchoring strength $W$ the first solution is slightly larger (in the sense that the actual angular jump in the solutions may be slightly more than $\pi$) and then zero, while the second one is slightly smaller then $\pi$. One notes that this limiting case itself is not realistic, but it enables one to obtain an analytical solution which will be used to develop a useful approximation for numerical curves.

Indeed, let us neglect the second term in equation (1.11). The corresponding first integral (1.12) can now be written in the simple form

$$W_s(\varphi) - K_w \frac{d}{2}\left(\frac{d\varphi}{dx}\right)^2 = C. \tag{1.17}$$

As discussed above, far from the wall the equilibrium angle is close either to 0 or to $\pi$ and therefore $W_s(\varphi) = -W$ far from the wall. Thus $C = -W$ and equation (1.17) can be rewritten in the following dimensionless form:

$$\sin^2\varphi = \left(\frac{d\varphi}{dX}\right)^2. \tag{1.18}$$

One notes that equation (1.18) is exactly the same as the one which describes the 'simple twist' director distribution near the surface [6], which is determined by a competition between surface alignment and the magnetic field, which is parallel to the surface but perpendicular to the easy axis. Very similar equations have also been obtained in the analyses of linear $2\pi$ solitons in polar smectic $C^*$ films in an external electric field [9, 10] and walls in freely suspended smectic $C$ films subject to magnetic fields [11].

As discussed above, in this case the limiting values for the equilibrium angle far from the wall are 0 and $\pi$. Thus in the middle of the wall $\varphi = \pi/2$. Introducing the angle $\Phi = \varphi - \pi/2$ and selecting, as before, the positive sign in the first derivative, one obtains

$$\frac{d\varphi}{dX} = \frac{1}{\sin\varphi}. \tag{1.19}$$

Equation (1.19) can be integrated using the substitution $t = \tan(\varphi/2)$. Then $\sin\varphi = 2t/(1+t^2)$ and $d\varphi = 2dt/(1+t^2)$. After substitution of these formulae into equation (1.19) one obtains $dX = dt/t$, which can be integrated to yield the solution $t = \exp(X) + t_0$. The integration constant $t_0$ is determined from the boundary conditions. At $X = +\infty$, $\varphi = \pi$ and therefore $t = +\infty$. At $X = -\infty$, $\varphi = 0$ and therefore $t = 0$. Thus $t_0 = 0$. As a result of this one obtains

$$\varphi = \arctan(\exp(X)). \tag{1.20}$$

Equation (1.20) presents the typical form of a $\pi$ wall [6, 9–11]. In our case it corresponds to an unrealistic limit, but the mathematical form of equation (1.20) can be used to compose an

analytical approximation for the actual solution, which can only be obtained numerically. In terms of the angle $\Phi$, the possible approximating function can be expressed as

$$\Phi = \Phi_e \left[ \frac{4}{\pi} \arctan(\exp(aX)) - 1 \right], \tag{1.21}$$

where $\Phi_e$ is the absolute value of the equilibrium angle far from the wall and $a$ is an unknown coefficient which is used as a free parameter to approximate the numerical curves. One can readily see that this simple approximation function is quite good and therefore can be used in other calculations to obtain more analytical results. This approximating function will be used in section 5 below to estimate the stationary velocity of the moving wall.

## 2. Wall profile for different anchoring potentials

In the preceding section we have used the widely accepted Rapini–Papoular anchoring potential. However, it has been shown recently [1, 2, 4, 5, 12] that in some phenomena connected with a pitch jump [1, 2, 4] or with the dynamics of a pitch jump [5, 12] in chiral liquid crystals the shape of anchoring potential may play an essential role because large angular deviations of the director from the alignment direction at the surface determine the characteristics of the corresponding phenomena. One may also expect quite essential dependence of the director distribution in the wall on the shape of the anchoring potential because inside the wall rather large deviations of the director from the alignment direction at the surface are present. This is why the structure of the wall for different model anchoring potentials is investigated in this section. Another reason for taking into consideration different forms of the anchoring potential is related to a significant sensitivity of the wall profile on the absolute value of the equilibrium angle $\varphi_e$ far from the wall. This angle is determined for a particular value of the temperature dependent parameter $\varphi_0(T)$ for which the free energies of the $N$ and $N+1$ configurations are equal. As discussed above, the equation for the angle $\varphi_e$ is obtained by minimization of equation (1.1) for $\varphi_0(T) = \pi/2$:

$$\frac{\partial}{\partial \varphi_e} W_s(\varphi_e) + \frac{1}{d} K_{22} \left( \varphi_e - \frac{\pi}{2} \right) = 0. \tag{2.1}$$

One can readily see from equation (2.1) that the equilibrium angle strongly depends on the anchoring strength $W$ and the cell thickness $d$. On the other hand, even with fixed values of these parameters the equilibrium angle also depends on the actual form of the anchoring potential $W_s(\varphi)$.

In this section we consider two very different model anchoring potentials: the standard Rapini–Papoular (RP) potential, given by [6, 7]

$$W_s(\varphi) = -\tfrac{1}{2} W \cos^2 \varphi, \tag{2.2}$$

and that recently introduced as the so-called B-potential [2], which is given by the formula

$$W_s(\varphi) = -W \left[ \cos^2 \left( \frac{\varphi}{2} \right) - \frac{1}{2} \right], \qquad \text{if } -\frac{\pi}{2} < \varphi < \frac{\pi}{2}. \tag{2.3}$$

Schematic pictures of these potentials are shown in figure 2. The B-potential also has period $\pi$, i.e. $W_s(\varphi + \pi) = W_s(\varphi)$. It is interesting to compare the values of the equilibrium angle $\varphi_e$ for the two different model potentials and for the same value of the parameter $S_d$. In figures 3 and 4 we present the values of $\varphi_e$ calculated for the two model potentials as a function of the parameter $S_d$ and the layer thickness, respectively (bold lines correspond to the RP potential). One notes that for the RP potential the director is inside the potential well at $\varphi_0(T) = \pi/2$ only if $S_d$ is less than one. For larger values of $S_d$ the director orientation remains unchanged, i.e. the

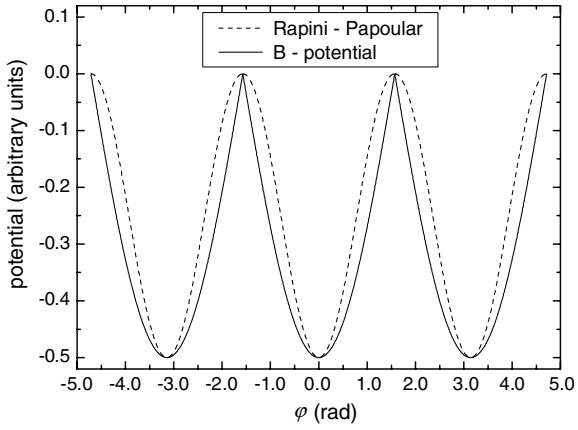


**Figure 2.** Qualitative plots of the RP potential and B-potential given by equations (2.2) and (2.3), respectively.

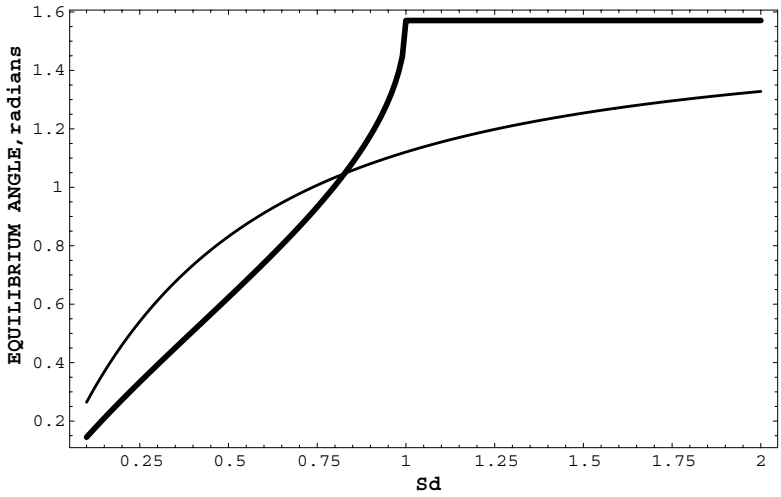


**Figure 3.** Director deviation angle (from the rubbing direction) $\varphi_e$ calculated as a function of the parameter $S_d$ for the temperature corresponding to equal free energies of the configurations with $N$ and $N+1$ director half-turns at the layer thickness for the RP potential (bold line) and B-potential.

angle $\varphi$ takes the value $\varphi_0(T) = \pi/2$ as shown in figure 3. This means that the equilibrium wall does not exist for $S_d > 1$ because in this case the two different equilibrium states, which may be separated by the wall, simply do not exist and there are no pitch jumps. In contrast, for the B-potential the equilibrium wall exists for any value of $S_d$. This essential difference between the RP and B-potentials is related to their different properties around the point of maximum at $\varphi = \pi/2$. The RP potential is everywhere smooth and has a negative curvature for $-W$ at the point of the maximum. In contrast to this, the B-potential has a discontinuous first derivative at the maximum point, and thus the curvature is infinitely large. One notes that the B-potential is a simple model for a class of possible potentials with a very sharp maximum (i.e. very large but finite curvature at the maximum point). For such potentials the large curvature at the maximum point guarantees the existence of the wall for a very broad range of parameters. This enables

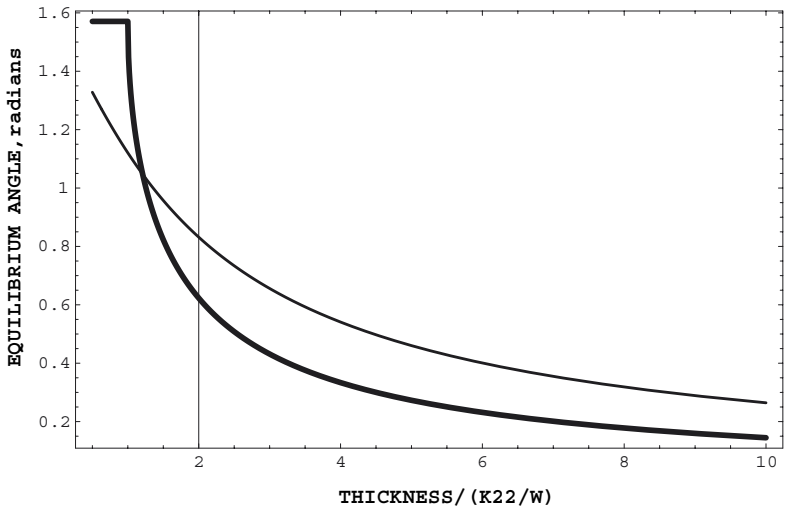


**Figure 4.** Director deviation angle $\varphi_e$ calculated as a function of the sample thickness normalized by the penetration length $K_{22}/W$ (other conditions are the same as in figure 3).

one to distinguish the B-type potentials among other possible potentials because only for the B-type potentials does an equilibrium wall exists for any thickness of the layer. For RP-type potentials an equilibrium wall exists if the layer is thick enough.

The difference between the two potentials can also be outlined by considering the stability of the wall. It should be noted here that the wall is always globally unstable because the total free energy of the cell with a wall is always higher then the free energy of the homogeneous cell in which the angle $\varphi$ is equal to the same equilibrium value everywhere in the cell. However, the wall may be metastable locally. This kind of stability can be checked by considering the stability of the state with $\varphi = \varphi_0(T) = \pi/2$, which may compete with the two energetically equivalent states with $\varphi = \pm\varphi_e$ separated by the wall. The stability of this state is determined by the sign of the second derivative of the free energy (1.1) calculated at $\varphi = \varphi_0(T) = \pi/2$. For example, for the RP potential

$$\left.\frac{d^2F}{d\varphi^2}\right|_{\varphi=\frac{\pi}{2}} = -W(1 - S_d). \tag{2.4}$$

Thus the state with $\varphi = \varphi_0(T) = \pi/2$ is always unstable if $S_d < 1$. This is the same criterion as the one derived above for the very existence of the wall. Thus for $S_d < 1$ the wall is locally stable because the two states with $\varphi = \pm\varphi_e$ are stable while the alternative state with $\varphi = \varphi_0(T) = \pi/2$ is unstable.

To obtain some general view of the shape of a motionless wall it is appropriate to consider in more detail the simple approximations involving equation (1.11) for the director distribution in the wall. To compare the director distribution in the wall for very weak anchoring and sufficiently strong anchoring ($S_d < 1$ in equation (1.21)) the angular distributions of the director in the wall in a 'dimensionless' representation are given in figure 5. The term 'dimensionless' means, in this context, that the angular deviations of the director are normalized by the complete angular change of the director orientations at the wall, and the coordinate perpendicular to the wall, $x$, is normalized by the wall thickness. Figure 5 shows that the 'dimensionless' distributions obtained for a weak anchoring and a strong anchoring from equation (1.11) are virtually indistinguishable. However, of course, the real distributions are also different in the

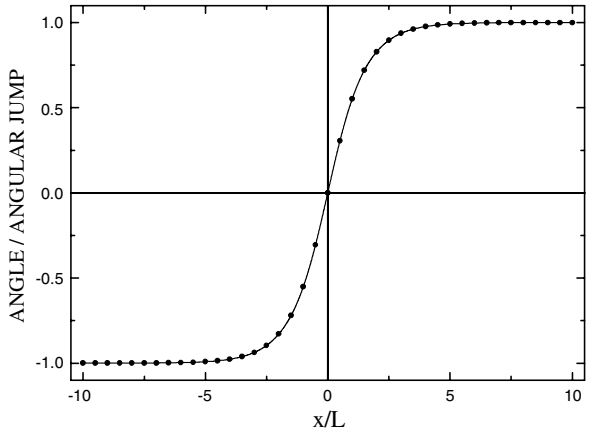


**Figure 5.** Dimensionless angular distribution (the angle normalized by the width of the jump and the coordinate normalized by the wall thickness) of the director at the layer surface with a finite anchoring in the wall for a weak anchoring (points) and a sufficiently strong anchoring (solid line).

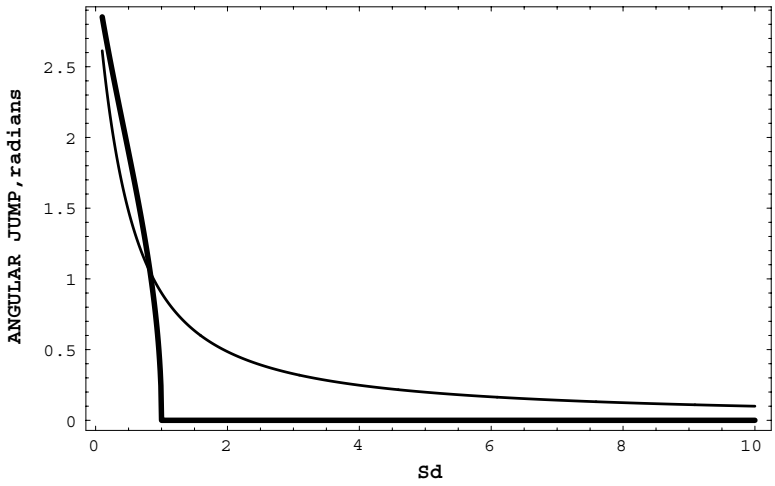


**Figure 6.** Angular jump of the director at the wall as a function of the parameter $S_d$ for the RP (bold line) and B-surface anchoring potentials.

wall thickness and similarly so in the complete angular change of the director orientations at the wall (see equation (1.16)). To obtain the actual shape of the wall from the shape of the dimensionless one it is sufficient to take into account figures 6 and 7, where calculated results are presented for the angular jump of the director at the wall as a function of the parameter $S_d$ and the layer thickness $d$, respectively, for RP and B-surface anchoring potentials. In particular, figure 6 shows that the wall cannot exist for the RP potential if $S_d > 1$, in contrast to the case for the B-potential, in which the wall exists for any value of the parameter $S_d$.

## 3. Stability of wall

As discussed in section 1, the description of the wall in a cholesteric cell considered in this paper is mathematically similar to the theory of walls created by a magnetic field. In the present

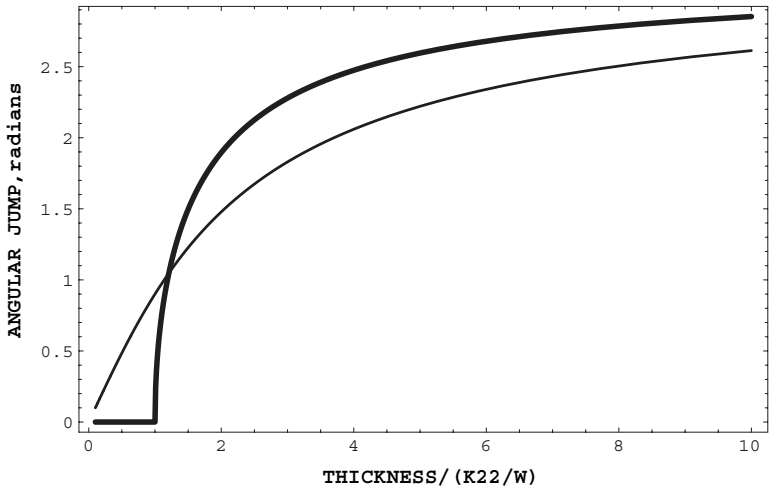


**Figure 7.** Angular jump of the director at the wall as a function of the layer thickness $d$ for the RP (bold line) and B-surface anchoring potentials.

system the anchoring potential in equation (1.1) is analogous to the interaction energy of the nematic director and the magnetic field. It is well known in other systems that by increasing the magnitude of the magnetic field the distortions inside the wall become increasingly larger and finally, at a certain field strength, a set of disclination lines appear [6, section 4.4.3]. Thus it is also reasonable to expect a transformation of the wall into disclination lines in thin cholesteric cells with sufficiently strong anchoring. To check the stability of the wall relative to a disclination one has to compare the energies of the wall and the disclination.

The energy of the wall $E_w$ is given by the following expression:

$$E_w = \int [F(\varphi(x)) - F_e]\mathrm{d}x. \tag{3.1}$$

In our approximation we know that the first integral of equation (1.11) is just equal to $F_e$. As a result, equation (3.1) may be rewritten, with the help of equation (1.17), in the form

$$E_w = \int \left[ \frac{K_w d}{2W} \left( \frac{\mathrm{d}\varphi}{\mathrm{d}x} \right)^2 \right] \mathrm{d}x. \tag{3.2}$$

In our static problem, $E_w$ may be easily expressed via the so-called dissipation integral [5]. This integral is represented by the formula

$$V = \int \left( \frac{\mathrm{d}}{\mathrm{d}x} \psi(x, z) \right)^2 \mathrm{d}z\, \mathrm{d}x, \tag{3.3}$$

which was investigated in [5] for the quasistatic approximation (which in our case is exact). If one uses the expression (1.6) connecting the derivative of angle $\psi$ with the derivative of $\varphi$ determining the director orientation at the surface of the layer then the dissipation integral accepts the following form:

$$V = \frac{d}{3} \int \left( \frac{\mathrm{d}\varphi}{\mathrm{d}x} \right)^2 \mathrm{d}x. \tag{3.4}$$

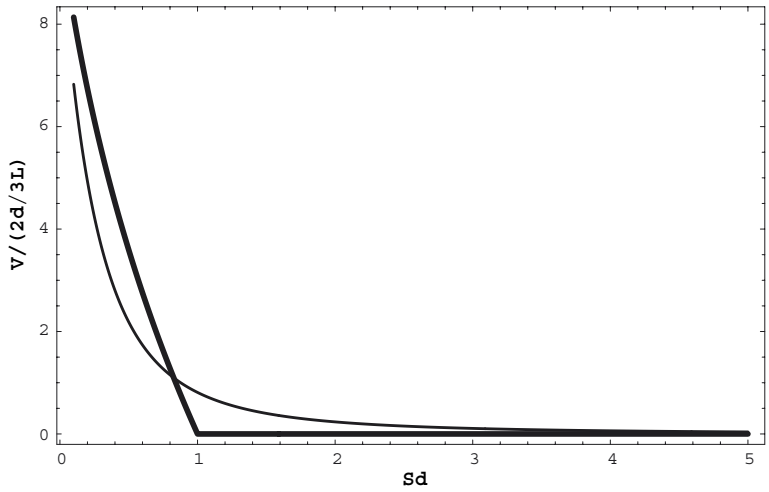


**Figure 8.** Dissipation integral (divided by $2d/3L$) as a function of the parameter $S_d$ for RP (bold line) and B-surface anchoring potentials calculated for the director distribution presented by equation (1.20).

The expression (3.2) for the energy of the wall per unit length normalized by the surface anchoring energy (per unit area) differs from the dissipation integral only by a coefficient, i.e.,

$$E_w = \frac{3}{2}\frac{K_w}{W}V. \tag{3.5}$$

This means that, in conventional units, $E_w = 3K_wV/2$. Therefore we have to compare the expression (3.5) with the energy of a disclination to find the range of related parameters where the wall is stable. In other words, we have to calculate the dissipation integral presented by formulae (3.4) for the director distributions in the wall calculated in the previous two sections.

In the one constant approximation for the liquid crystal elastic moduli, $K_{11} = K_{22} = K_{33} = K$, the disclination energy $T$ per unit length is estimated [6, 7, 13] as $\pi K m^2 \ln(\rho_{max}/a)$ where $m$ is the strength of the disclination and the logarithmic factor, which weakly depends on the other parameters, is of the order 10 [6, p 171].

In the general case, calculation of the dissipation integral (3.3) demands a numerical approach. However, the dissipation integral can be estimated using the analytical approximating function (1.21). After straightforward integration one obtains the estimate

$$V = \frac{2d}{3L}\left(1 - \frac{2}{\pi}\varphi_e\right)^2. \tag{3.6}$$

In equation (3.6) the effective width of the wall $L$ is of the order $L = (W/K_wd)^{-1/2}$. In the one constant approximation $K_w \approx K/2$ the factor $d/L$ in equation (3.6) can be estimated as $d/L \approx S_d^{-1/2}$. Finally, the energy of the wall per unit length is estimated as $E_w \approx (1 - 2\varphi_e/\pi)^2 K S_d^{-1/2}$. This estimate should be compared with the estimate for the energy of a disclination line $E_d \approx 10\pi K$ where we have taken $m = 1$. One concludes that the continuous wall is stable against a set of disclination lines if $(1 - 2\varphi_e/\pi)^2 K S_d^{-1/2} \leqslant 10\pi$. One notes that this criterion is very sensitive to the value of the equilibrium angle $\varphi_e$, which in turn depends on the parameter $S_d$ and on the actual shape of the anchoring potential. The dependence of the factor $(1 - 2\varphi_e/\pi)^2 K S_d^{-1/2}$ on the parameter $S_d$ is presented in figure 8

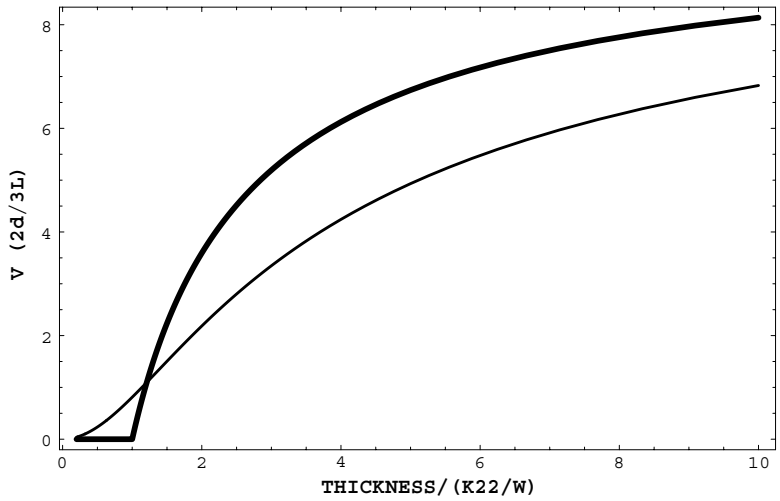


**Figure 9.** Dissipation integral (divided by $2d/3L$) versus the layer thickness (normalized by the penetration length $L_{\mathrm{p}} = K_{22}/W$) for RP (bold line) and B-surface anchoring potentials calculated for the director distribution given by equation (1.20).

for RP and B-potentials. The same integral as a function of the layer thickness is presented in figure 9. One concludes that energy of the wall is smaller than that of the disclination lines if $S_{\mathrm{d}}$ is sufficiently large. One can readily see that the dimensionless energy of the wall is less than $10\pi K$ for $S_{\mathrm{d}} > 0.1$. Qualitatively, this means that the stable wall cannot be too narrow compared to the cell thickness $d$. The thickness of the wall is typically smaller than $d$.

## 4. Motion of a planar wall

In the previous sections we have considered the structure of the equilibrium nonsingular wall which separates the regions of different cholesteric pitch. As discussed above, the motionless equilibrium wall may exist only if the free energies in the two different regions are the same. However, if the free energies are different then the wall begins to move, driven by the generalized thermodynamic force proportional to the free energy difference $\Delta F = F(\varphi_{\mathrm{e}1}) - F(\varphi_{\mathrm{e}2})$. Movement of the wall has indeed been observed in experiments [14, 15]. Moreover, it is, in fact, much more difficult to observe the stationary wall because this requires a number of special experimental conditions. In an ideal system the wall may be planar and move with a certain stationary velocity $v_{\mathrm{s}}$. In this section we consider the dynamics of the wall in the simplest planar case. The general equation for the stationary velocity of the domain wall can be derived using energy conservation arguments presented, for example, in [5].

Let us assume that the planar wall which separates the regions with free energy densities $F_{\mathrm{I}}/d$ and $F_{\mathrm{II}}/d$ (obtained from the free energy as defined in equation (1.1)) is moving with constant velocity $v_{\mathrm{s}}$ in the direction perpendicular to the wall. During time $\mathrm{d}t$ the wall covers the distance $\mathrm{d}x = v_{\mathrm{s}}\mathrm{d}t$. Consequently, the infinitesimal change of the total free energy $F_V$ of the cell is

$$\mathrm{d}F_V = ((F_I - F_{II})/d)\mathrm{d}V = (S\Delta F/d)v_{\mathrm{s}}\mathrm{d}t, \tag{4.1}$$

which gives an equation for the free energy per unit length of the form [8]

$$\frac{\mathrm{d}F'}{\mathrm{d}t} = \Delta F v_\mathrm{s}, \tag{4.2}$$

where $\mathrm{d}F' = \mathrm{d}F_V\, d/S$. It has been shown by the authors in a previous paper [12] that the rate of change of the free energy of the cell is given by following general equation:

$$\frac{\mathrm{d}F'}{\mathrm{d}t} = -\int D\,\mathrm{d}x\,\mathrm{d}z, \tag{4.3}$$

where the dissipation function $D$ is expressed as

$$D = \gamma_1 \left(\frac{\mathrm{d}\phi}{\mathrm{d}t}\right)^2. \tag{4.4}$$

In the stationary case the profile of the wall is preserved and the angle $\phi(x)$ should be given by a travelling wave solution of the type $\phi(x - v_\mathrm{s}t)$. In this case one obtains

$$\frac{\mathrm{d}F'}{\mathrm{d}t} = -\gamma_1 (v_\mathrm{s})^2 \int \left(\frac{\mathrm{d}\phi}{\mathrm{d}x}\right)^2 \mathrm{d}x\,\mathrm{d}z. \tag{4.5}$$

Similar to the previous work in this paper and [12], we assume that the director profile is everywhere quasistatic, i.e. $\phi(z, x, t) = (z/d)\phi(x, t)$. Substituting this expression into equation (4.5) one obtains

$$\frac{\mathrm{d}F'}{\mathrm{d}t} = -\frac{1}{3}\mathrm{d}\gamma_1 (v_\mathrm{s})^2 \int \left(\frac{\mathrm{d}\phi}{\mathrm{d}x}\right)^2 \mathrm{d}x. \tag{4.6}$$

Comparing equations (4.2) and (4.6) one finally obtains the general expression for the stationary velocity $v_\mathrm{s}$ given by

$$v_\mathrm{s} = -3\frac{\Delta F}{\mathrm{d}\gamma_1 \int (\frac{\mathrm{d}\phi}{\mathrm{d}x})^2 \mathrm{d}x}. \tag{4.7}$$

One notes that the integral in the denominator of equation (4.7) is the dissipation integral discussed above.

Now let us rewrite equation (4.7) in dimensionless form. The free energy difference $\Delta F$ has the same dimension as the quantity $K_{22}/d$ and thus $F$ can be normalized by $K_{22}/d$. Also, introducing the dimensionless coordinate $x' = x/d$ and dimensionless time $\tau = t/\tau_0$ where $\tau_0 = \gamma_1 d^2/3K_{22}$ is the unit of time used in [12], one obtains the equation for the dimensionless velocity $v'_\mathrm{s}$:

$$v'_\mathrm{s} = -\frac{\Delta \tilde{F}}{\int (\frac{\mathrm{d}\phi}{\mathrm{d}x'})^2 \mathrm{d}x'}. \tag{4.8}$$

If the free energy difference $\Delta\tilde{F}$ is small and the parameter $S_\mathrm{d} \sim 1$, the difference can be estimated as $\Delta\tilde{F} \sim \Delta\phi_\mathrm{e}$ where $\Delta\phi_\mathrm{e} \ll \phi_\mathrm{e}$ is the difference in the equilibrium anchoring angles in the two regions. The so-called dissipation integral is $\int (\frac{\mathrm{d}\phi}{\mathrm{d}x'})^2 \mathrm{d}x' \sim (d/L) \gg 1$, where $L$ has the meaning of the thickness of the wall, which is typically smaller then the cell thickness. As a result, the dimensionless velocity $v'_\mathrm{s}$ can roughly be estimated as

$$v'_\mathrm{s} \sim \Delta\phi_\mathrm{e}\frac{L}{d} \ll 1. \tag{4.9}$$

It is important to note that the dimensionless velocity is small, i.e. $v'_\mathrm{s} \ll 1$, due to the factor $L/d \ll 1$, even if the difference in angles $\Delta\phi_\mathrm{e}$ is not really small.

In equation (4.9) the stationary velocity depends on the profile of the wall $\phi(x)$. One notes that in the general case the profile of the moving wall differs from that of the equilibrium one

because it depends on the velocity of the wall. The equation for the profile of the moving wall can be derived in the following way. According to [12], the dynamics of the azimuthal angle $\phi(x)$ is described by the following equation:

$$\frac{\mathrm{d}\phi}{\mathrm{d}t} = -\frac{3}{\gamma_1 d}\frac{\partial F_\mathrm{d}}{\partial \phi}, \tag{4.10}$$

where $F_\mathrm{d}$ is the free energy density of the system. Inside the wall the free energy density is given by equation (1.11), which takes into account the inhomogeneous profile of the angle $\phi(x)$. Substituting (1.11) into equation (4.10) one obtains a differential equation for the function $\phi(x, t)$:

$$\frac{\mathrm{d}\phi}{\mathrm{d}t} = -\frac{3}{\gamma_1 d}\left[\frac{\mathrm{d}}{\mathrm{d}\phi}W_\mathrm{s}(\phi) + \frac{1}{d}K\,(\phi - \phi_0(T)) - K_\mathrm{w} d\,\frac{\mathrm{d}^2\phi}{\mathrm{d}x^2}\right]. \tag{4.11}$$

Taking into account again that $\phi = \phi(x - v_\mathrm{s}t)$, the time derivative $\mathrm{d}\phi/\mathrm{d}t$ can be rewritten as $-v_\mathrm{s}(\mathrm{d}\phi/\mathrm{d}x)$. Now the stationary profile $\phi(x)$ is a solution of the following equation which depends on the stationary velocity $v_\mathrm{s}$:

$$-v_\mathrm{s}\frac{\mathrm{d}\phi}{\mathrm{d}x} = -\frac{3}{\gamma_1 d}\left[\frac{\mathrm{d}}{\mathrm{d}\phi}W_\mathrm{s}(\phi) + \frac{1}{d}K\,(\phi - \phi_0(T)) - K_\mathrm{w} d\,\frac{\mathrm{d}^2\phi}{\mathrm{d}x^2}\right]. \tag{4.12}$$

In the general case, equations (4.8) and (4.12) should be solved together to calculate both the actual profile of the moving wall and the stationary velocity. Note also that the velocity can be estimated from (4.12) if the velocity in (4.7) can be calculated. It can be shown, however, that the difference between the profiles of the stationary and moving walls is small because of the smallness of the dimensionless velocity. Thus the velocity of the wall can be estimated using the general equation (4.12) and a suitable equilibrium profile calculated for $v_\mathrm{s} = 0$. The correction determined by the difference between the two profiles is quadratic in the small dimensionless velocity $v_\mathrm{s}'$. In practice we split the dissipation integral into two parts which correspond to the domains of positive and negative $x$, respectively. One of these integrals is calculated numerically using the equilibrium profile which depends on the equilibrium angle $\phi_{\mathrm{e}1}$ on one side of the wall, while the second integral is calculated using the second equilibrium profile which depends on $\phi_{\mathrm{e}2}$. In this way we account approximately for the asymmetry of the moving wall.

The quantity which may be directly measured in an experiment is the temperature dependence of the velocity $v_\mathrm{s}$. The range of temperatures where these measurements have to be carried out spreads from the temperature corresponding to equal free energies of the $N$ and $N + 1$ configurations in the layer which corresponds to zero velocity $v_\mathrm{s}$ and director deviation angle at the surface equal to $\varphi_\mathrm{e}$, up to the temperature of absolute instability of the $N$ configuration, which corresponds to the maximum of velocity $v_\mathrm{s}$ and director deviation angle at the surface equal to the critical angle $\varphi_\mathrm{c}$. These two points correspond to quite definite values of the pitch in a bulk cholesteric (it is assumed that the pitch is temperature dependent). However, it is more convenient to use the parameter $\varphi_0(T)$ which is temperature dependent and which is directly related to the pitch ($\varphi_0(T) = 2\pi d/p(T) - \pi\,\mathrm{Int}[2d/p(T)]$, where $p(T)$ is the temperature dependent pitch in a bulk cholesteric). At the temperature that ensures equal free energies of the $N$ and $N+1$ configurations, $\varphi_0 = \pi/2$. At the absolute instability point of the $N$ configuration the value of $\varphi_0 = \varphi_{0c}$ depends on the strength and shape of the anchoring potential and is expressed via the critical angle $\varphi_\mathrm{c}$.

For a comparison with future experimental data it is convenient to present the temperature variations of the velocity $v_\mathrm{s}$ normalized by the velocity calculated for some characteristic temperature, for example for the temperature of absolute instability of the $N$ configuration

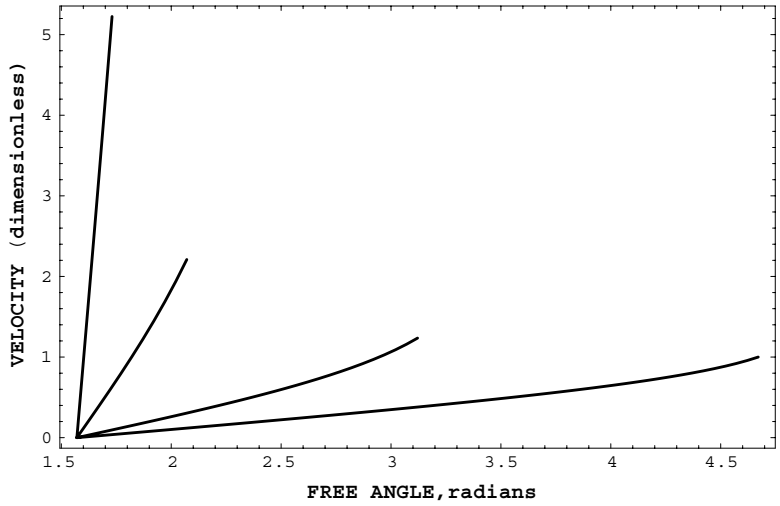


**Figure 10.** The calculated flat wall velocity as a function of temperature (free rotation angle), for the B-potential at $S_d = 1/2\pi$, $1/\pi$, 1 and 3 (normalized by the velocity at the critical free rotation angle for $S_d = 1/2\pi$).

$T_c$ (which corresponds to $\varphi_0 = \varphi_{0c}$, as discussed above). One obtains from equation (4.7)

$$\frac{v_s(T)}{v_s(T_c)} = \frac{\Delta F(T)}{\Delta F(T_c)} \frac{V(T_c)}{V(T)}, \tag{4.13}$$

where $\Delta F(T)$ is the temperature dependent difference of the free energies of the layer for the $N$ and $N+1$ configurations and $V(T)$ is the temperature dependent dissipation integral determined from equation (3.3). The first factor on the right-hand side of equation (4.13) can be calculated exactly by using equation (1.1) for the free energy of the layer as a function of $\varphi_0$. The second factor on the right-hand side of equation (4.13) may be estimated using equation (3.6), where the factor $\pi(1 - 2\varphi_e/\pi)$ (which is the change of the angle across the equilibrium wall) should be replaced by the corresponding temperature dependent jump $\Delta\varphi(T)$, which has to be calculated using the free energy (1.1) and may be presented as a function of $\varphi_0$. Finally, the ratio of the velocities at temperatures $T$ and $T_c$ can be estimated as

$$\frac{v_s(T)}{v_s(T_c)} = \frac{\Delta F(T)}{\Delta F(T_c)} \left[\frac{\Delta\varphi(T_c)}{\Delta\varphi(T)}\right]^2 \frac{L(T)}{L(T_c)}. \tag{4.14}$$

In equation (4.14) the effective thickness of the wall $L(T)$ is generally temperature dependent and unknown. The ratio $L(T)/L(T_c)$, however, is expected to be of the order of unity and thus the corresponding dependence can be neglected in a first approximation. The temperature variation of the dimensionless velocity, i.e. $v_s(T)/v_s(T_c)$, calculated for the B- and RP potentials using equation (4.14) for $L(T)/L(T_c) = 1$, are presented in figures 10 and 11, respectively.

The possible deviations of the experimentally measured velocity $v_s(T)$ from the calculated one (using equation (4.14) with $L(T)/L(T_c) = 1$) will be an indication of the temperature dependence of the effective thickness $L(T)$ of the moving wall because in the expression for the ratio of the measured velocity to the calculated one the factor $L(T)/L(T_c)$ is no longer constant but will be temperature dependent. One expects that some temperature variation of the effective thickness of the moving wall does exist, but it should not be too strong. In this

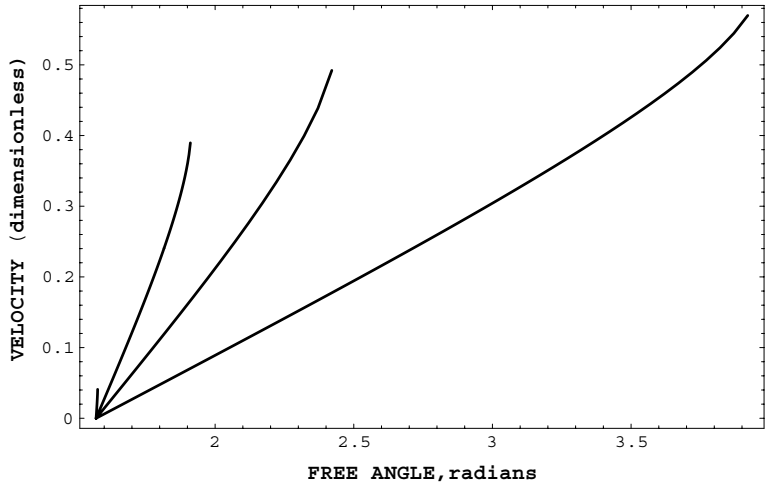


**Figure 11.** The calculated flat wall velocity as a function of temperature (free rotation angle), for RP potential at $S_d = 1/2\pi, 1/\pi, 0.5$ and 0.95 (normalized by the velocity at the critical free rotation angle for $S_d = 1/2\pi$ for the B-potential).

way one may estimate the temperature variation of the effective thickness of the wall without extensive numerical calculations.

The calculations presented in figures 10 and 11 show the temperature dependences of the flat wall velocity and reveal the essential difference between the RP and B-potentials. These figures show that the velocity of the flat wall for the same value of $S_d$ is significantly higher for the B-potential. The dependences of the flat wall velocity on the layer thickness and the parameter $S_d$ are also quite different for the RP and B-potentials. The absolute value of the maximal flat wall velocity $v_s(T_c) = v_s(\varphi_e)$ (see [5]), for the layer thickness $d = 5\ \mu$m and typical values for $K_{22}$, $\gamma_1$ [6] with $S_d \approx 1/2$ for the B-potential is approximately equal to 2 mm s$^{-1}$, and it is 10 to 15 times less for the RP potential. The velocity is decreasing with increasing layer thickness for both model potentials. This means that experimental investigations of the motion of the wall may be used to distinguish between possible different shapes of the surface anchoring potential.

## 5. Conclusions

The results of the previous sections show that the distribution of the director in the wall is directly dependent on the characteristics of the surface anchoring potential. The proposed analytical expressions for the wall profile may be regarded as initial approximations for the numerical calculation of the director distribution in the wall and in the fitting of theory to experiments. It is essential that the corresponding fitting for different model anchoring potentials may yield some information about the actual shape of the surface anchoring potential. Optical measurements at the wall appear to be the most relevant and simple kind of measurements for the determination of the director distribution in the wall.

The director distributions in the wall determined above are useful for describing the pitch jump dynamics, namely, the motion of the interface between regions with different values of the pitch [5]. The described motionless wall remains motionless only at unchanged values of the physical parameters, for example the temperature. If the temperature (being the parameter $\varphi_0(T)$ in the equations) changes, then the free energies of the director configurations at opposite

sides of the wall cease to be equal and the wall begins its motion in the direction of the higher free energy side. Therefore, in any case, for a small velocity in this motion the director distribution in the wall is weakly disturbed by the motion and as a good approximation for a slowly moving wall we may accept the distribution found above.

For the director distribution in a moving wall in the general case the corresponding problems that occur are much more complicated (see, for example, the similar problem of wall motion in nematics under an applied external field [16]). Generally speaking, the full problem demands the application of a numerical approach for finding the solution of the corresponding nonlinear equations, and only under rather strongly accepted assumptions [16] can one hope to reduce the problem to nonlinear equations with known solutions.

The calculation for the velocity of the straight interface performed above, under the assumption that the shape of a moving wall is the same as that for a motionless wall, may be regarded as a guide for the experimental investigations of nonsingular walls, their motion being connected to the specific shape of the surface anchoring potential. Several authors have reported on the observation and motion of such walls in chiral liquid crystals [17, 18]; however, there have as yet been no reports on the systematic study of such related phenomena. The work contained in [4], where similar walls and their motion were observed in nematic materials via mechanical twisting of a nematic layer, deserves a special mention because, in some aspects, the study of walls under mechanical twisting looks more tractable than the corresponding study for cholesterics under temperature variations.

## Acknowledgments

The authors are grateful for the UK EPSRC grant GR/S34311/01 that enabled this work to be undertaken. Useful discussions of the considered problems with E Kats, P Oswald, W Kuczynski, H Gleeson, H Coles, M Pivnenko and the partial funding of this work by the RFBR (grant N 06-02-16287) are greatly appreciated by VAB.

## References

[1] Belyakov V A, Oswald P and Kats E I 2003 *JETP* **96** 915
[2] Belyakov V A, Stewart I W and Osipov M A 2004 *JETP* **99** 73
[3] Kim J H, Yoneya M and Yokoyama H 2002 *Nature* **420** 159
[4] Belyakov V A and Kuczynski W 2005 *Mol. Cryst. Liq. Cryst.* **438** 123
[5] Belyakov V A, Oswald P and Kats E I 2006 *JETP* at press
[6] de Gennes P G and Prost J 1993 *The Physics of Liquid Crystals* 2nd edn (Oxford: Oxford University Press)
[7] Oswald P and Pieranski P 2000 *Les Cristaux Liquides: Concepts et Propriétés Physiques Illustrées par des Expériences* (Paris: Gordon and Breach)
[8] Belyakov V A and Kats E I 2000 *JETP* **91** 488
[9] Pindak R, Young C Y, Meyer R B and Clark N A 1980 *Phys. Rev. Lett.* **45** 1193
[10] Link D R, Radzihovsky L, Natale G, Maclennan J E, Clark N A, Walsh M, Keast S S and Neubert M E 2000 *Phys. Rev. Lett.* **84** 5772
[11] Dolganov P V and Bolotin B M 2003 *JETP Lett.* **77** 503
[12] Belyakov V A, Stewart I W and Osipov M A 2005 *Phys. Rev.* E **71** 051708
[13] Smalyukh I I and Lavrentovich O D 2002 *Phys. Rev.* E **66** 051703
[14] Coles H C 2004 private communication
[15] Kuczynski W 2005 private communication
[16] Cladis P E and van Saarloos W 1992 *Solitons in Liquid Crystals* ed L Lam and J Prost (New York: Springer) pp 110–50
[17] Gleeson H F 2004 private communication
[18] Pivnenko M N 2004 private communication